Int. J. Electrochem. Sci., 17 **(2022)** Article Number: 220850, doi: 10.20964/2022.08.46

International Journal of
ELECTROCHEMICAL
SCIENCE
www.electrochemsci.org

Effect of Different Surface Treatments of 42CrMo Steel Piston Rod on its Corrosion Resistance in Sodium Chloride Solution

Yihong Zhao[*], *Kai Wang*[*], *Zili Wang, Minjie Shi, Fangfang Li, Chengcong Ye*

School of Mechanical Engineering, Yangzhou University, Yangzhou, 225127, China.
[*]E-mail: yihongzhao99@sina.com, wk5962040@163.com

Received: 9 April 2022 / *Accepted:* 17 June 2022 / *Published:* 4 July 2022

42CrMo has good hardenability, high temperature strength and creep resistance, and is widely used in the manufacture of piston rod and other parts. Piston rod is the core moving part of automobile shock absorber, the failure of shock absorber will affect the performance of the entire automobile suspension system, and has a great threat to the safety of automobile driving. Therefore, improving the surface corrosion resistance of piston rod has important practical significance. In this paper, the piston rod surface was strengthened by trivalent chromium electroplating technology and gas oxy-nitriding composite treatment technology, and 42CrMo steel was used as the matrix material of the piston rod to study the corrosion resistance of the sample with electrochromium plating and gas oxy-nitriding composite treatment. The modified layer was observed and characterized by IM3000 inverted metallographic microscope. The potentiodynamic polarization curves and electrochemical impedance spectrum of the samples were measured by GAMRY ESA410 electrochemical workstation to analyze their corrosion resistance. The results show that the total thickness of oxide layer and compound layer is 20.89 μm for GNO sample and 18.56 μm for GNPO sample. The compound layer has good anticorrosion effect. The corrosion resistance of the samples after the different processes in order of strength to weakness are GNPO sample, GNO sample, chrome-plated sample, nitriding sample and substrate. The E_{corr} of corrosion potential and I_{corr} of corrosion current density of GNPO sample are -363 mV and 0.89 μA/cm^2 respectively, showing the best corrosion resistance.

Keywords: 42CrMo; trivalent chromium electroplating technology; gas oxy-nitriding composite treatment; corrosion resistance.

1. INTRODUCTION

42CrMo has good hardenability, high temperature strength and creep resistance. It has excellent comprehensive mechanical properties after tempering, is widely used in the manufacture of bolts, key shafts and piston rods with wear and alternate loads during service. As the core moving parts of automobile shock absorber, the piston rod is usually treated by electroplating process. The piston rod

not only works in the sliding friction environment for a long time, but also is vulnerable to lateral load impact in the driving process, which will cause the brittle hard chrome coating on the piston rod surface to peel off, pits and bumps and other defects that harm the life of the shock absorber. On the one hand, these defects will aggravate the wear and even rupture of sealing elements, on the other hand, they will also accelerate the destruction of the piston rod surface, forming a vicious circle, and eventually make the oil seal failure, leading to oil leakage of the shock absorber and early failure [1]. The failure of the shock absorber will affect the performance of the entire automobile suspension system, which has a great threat to the safety of automobile driving. Therefore, it is of great practical significance to study how to improve the wear resistance and corrosion resistance of piston rod surface.

At present, many researchers have adopted a variety of technologies to strengthen the surface of the piston rod, including chrome plating, thermal spraying, laser cladding, nitriding and so on.

Chromium plating is a typical single metal coating and is now widely used in various industries as an electroplating technology. Chromium plating technology has been widely used in shock absorber piston rod surface enhancement treatment, its processing process can not eliminate environmental pollution, piston rod service process due to chromium coating peeling, convex and other factors caused by early seal failure of the problem of concern[2-4].

Nitriding can improve the wear and corrosion resistance of the workpiece and reduce the amount of deformation of the workpiece during processing. With the development of industrial technology, the comprehensive performance requirements of the surface of the parts are improved, in order to further improve the surface wear resistance and corrosion resistance, the oxidation process is used as the pre-treatment and post-treatment of the nitriding process, oxidation pre-treatment and post-treatment are defined as pre-oxidation and post-oxidation, respectively. So gas oxy-nitriding composite treatment is composed of three parts: pre-oxidation, nitriding and post-oxidation. In the process of oxygen and nitriding, the infiltration agent element in the gas penetrates into the interior and surface of the workpiece through decomposition, adsorption and diffusion. When nitrogen concentration is low, nitrogen atoms are absorbed by metal in the form of thermal diffusion to form nitrogen-containing solid solutions. After a certain gradient diffusion layer of nitrogen concentration is formed, the chemical diffusion of nitrogen occurs on the metal surface, and the compound layer of iron nitride is formed and thickened by diffusion[5-8]. Gas oxy-nitriding composite treatment technology can greatly improve the wear resistance and corrosion resistance of the surface of parts. Gas oxygen-nitriding technology is rarely used to improve piston rod performance

In this paper, the piston rod surface is strengthened by trivalent chromium electroplating technology and gas oxy-nitriding composite treatment technology, and 42CrMo steel is used as the piston rod matrix material to study the corrosion resistance of chromium plating and gas oxy-nitriding composite treatment sample.

2. EXPERIMENTAL

2.1 Sample Preparation

The test base material is 42CrMo steel tempered by induction heat treatment technology, quenched at 900 °C and tempered at 600 °C. The apparent Vickers hardness after tempering is

approximately 380 $HV_{0.1}$. The samples were machined to 12 mm × 12 mm × 8 mm using wire cutting, polished step by step by metallographic sandpaper to mirror surface, and finally placed in anhydride ethanol environment for ultrasonic washing and drying. Chromium plating technology and gas oxy-nitriding composite treatment technology were used to treat the matrix materials respectively.

The 42CrMo steel was treated by trivalent chromium solution electroplating process. The process route was oil removal—acid activation—cleaning—chromium plating—cleaning—drying. The specific process parameters are shown in Table 1.

Table 1. Trivalent chromium solution electroplating parameters

Main salt	Complexing agent	temperature /℃	PH	Current density A/dm^2
Chromium sulfate	glycine	15-55	1-4	3-100

For the gas oxy-nitriding composite treatment of 42CrMo steel, GNO(gas-nitridng-oxidizing) and GNPO(gas-nitridng-polishing-oxidizing) processes were adopted. GNO process route was pre-oxidation—two-stage nitridng—post-oxidation, GNPO process route was pre-oxidation—two-stage nitridng—polishing—post-oxidation. The only difference between the two processes is whether the samples are polished after nitriding.

The gas oxy-nitriding composite treatment was carried out in the covered nitriding furnace, and its oxidation and nitriding were treated in the same furnace, the equipment has a special intake and exhaust control system. First of all, water vapor was introduced for heating and preheating oxidation treatment, then the first stage of nitriding underwent strong permeation, so that the surface had a diffuse distribution of nitride particles, followed by the diffusion infiltration of the second stage of nitriding. After nitriding, the samples were cooled to 120 °C, the samples were removed from the furnace and subjected to unpolished and polished respectively. Finally, the unpolished and polished samples were post-oxidized. The process parameters are shown in Table 2, 3, 4. We can get nitriding samples(samples that are treated with pre-oxidation and two-stage nitridng), GNPO samples(samples that are polished after nitriding and finally oxidized) and GNO samples（samples that are directly oxidized after nitriding without polishing）.

Table 2. Pre-oxidation process parameters

Oxidation temperature /℃	Oxidation time /h	Water vapor flow kg/h
400	1	10

Table 3. Two-stage nitriding process parameters

First stage nitriding			Second stage nitriding		
temperature /℃	Time/h	NH_3:CO_2	temperature /℃	Time/h	NH_3:CO_2
600	3.5	12:1	500	1.5	24:1

Table 4. Post-oxidation process parameters

Oxidation temperature /℃	Oxidation time /h	Water vapor flow kg/h
500	2	10

2.2 Characterization

The EDM cutter was used to cut the sections of the oxygen-nitriding and chrome-plated samples, which were then sequentially ground with metallographic sandpaper and pre-grinding, and then polished to a mirror finish using a diamond spray polish. The modified layer was etched with 4% nitric acid alcohol solution for about 4 hours, and then the sample was put into alcohol for ultrasonic cleaning. The modified layer was observed and characterized by IM3000 inverted metallographic microscope.

The potentiodynamic polarization curves and electrochemical impedance spectrum(EIS) of the samples were measured by GAMRY ESA410 electrochemical workstation to analyze their corrosion resistance. The samples to be tested were working electrode, the platinum sheet was used as the counter electrode, and the saturated calomel electrode was used as the reference electrode and the effective exposure area was approximately 1 cm^2. The corrosion medium was 3.5%NaCl solution, and the solution temperature was kept at 25±5 ℃. After the open-circuit potential of the test sample is stabilized (the potential fluctuation is within 10 mV), the electrochemical impedance spectrum and potentiodynamic polarization curve are measured. Electrochemical impedance spectrum frequency range between 0.01 Hz and 10 KHz, selected relative to the open circuit potential -400 mV to 800 mV range, measured at a 10 mV/s scanning rate of potentiodynamic polarization curves.

3. RESULTS AND ANALYSIS

3.1 Micromorphology

Figure 1 (a), (b) and (c) show the sectional corrosion microscopic morphology of 42CrMo steel treated by different processes, Figure 1 (a) and (b) show GNPO and GNO samples respectively, Figure 1 (c) show the sectional morphology of chrome-plated steel. The surface of the trivalent chromium electroplating sample forms a bright white chromium coating of about 22 μm, and the boundary between the trivalent chromium electroplating sample and the substrate is clear and there are obvious gaps[9]. It can be seen from Figure 1 (a) and (b) that the permeable layer of GNPO and GNO samples are composed of oxide layer, compound layer (white bright layer) and diffusion layer, and the black permeable layer in contact with aluminum foil is oxidized layer. The total thickness of oxide layer and compound layer of GNO sample is 20.89 μm, and that of GNPO sample is 18.56 μm. The compound layer has improved wear and corrosion resistance.

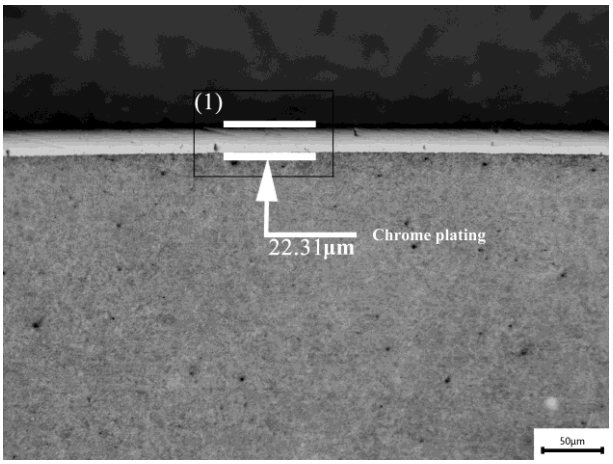

(a)Chrome-plated sample

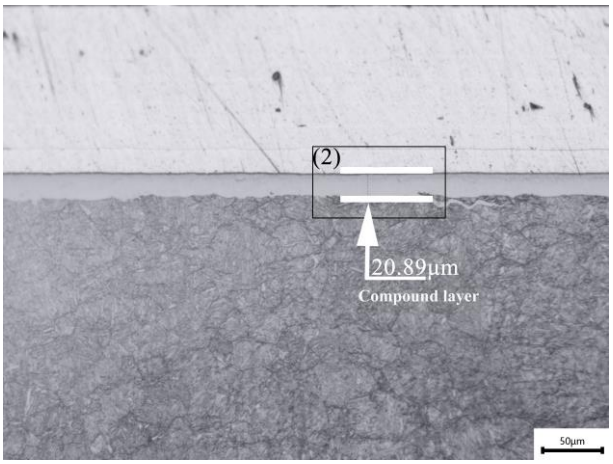

(b)GNO sample

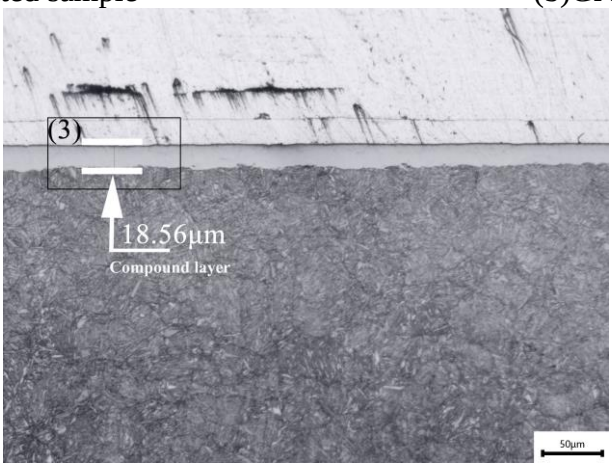

(C)GNPO sample

Figure 1. Microscopic morphology of the modified layer (Magnification: 200x)

3.2 Electrochemical performance test and analysis

3.2.1 Open circuit potential

Figure. 2 shows the open circuit potential curves of five samples immersed in 3.5%NaCl solution treated with different processes. On the one hand, it can be seen from the figure that at the initial stage of immersion, the open-circuit potential of five samples show a rapid negative shift, which is mainly due to the oxidation of exposed metal on the anode surface of the sample as the working electrode, resulting in the accumulation of a large number of negative charges on the surface of the working electrode, resulting in negative potential shift. After immersion for a certain period of time, the open-circuit potential curves of the two samples treated by gas oxygen-nitridation show repeated positive and negative fluctuations, which is due to the imbalanced charge distribution on the electrode surface due to the existence of pores on the oxide layer, which continuously affected the potential change. After 1800 s, the charge transfer is inhibited by passivation or corrosion products on the electrode surface. The whole electrode system is in a state of dynamic equilibrium, and the open circuit potentials of all samples tend to be stable. On the other hand, GNPO sample has the most positive open-circuit potential in the figure due to the protective effect of oxide film and compound layer, so it

has the minimum thermodynamic tendency of corrosion. The open circuit potential of the GNO sample is slightly lower than that of the GNPO sample, which is due to the fact that the GNO sample is not polished and its oxide layer is uneven and dense. Although the open-circuit potential of nitriding sample is lower than that of oxygen-nitriding composite treatment sample, the potential value is still higher than that of chrome-plated sample. Because Cl^- ions in solution can not penetrate the dense layer of ferro - nitrogen compound to reach the matrix, but can contact with the matrix through cracks on the surface of the chrome-plated coating, the chrome-plated sample has a thermodynamic tendency of corrosion second only to the matrix. Without the protection of any modified layer, the substrate has the greatest thermodynamic tendency of corrosion[10].

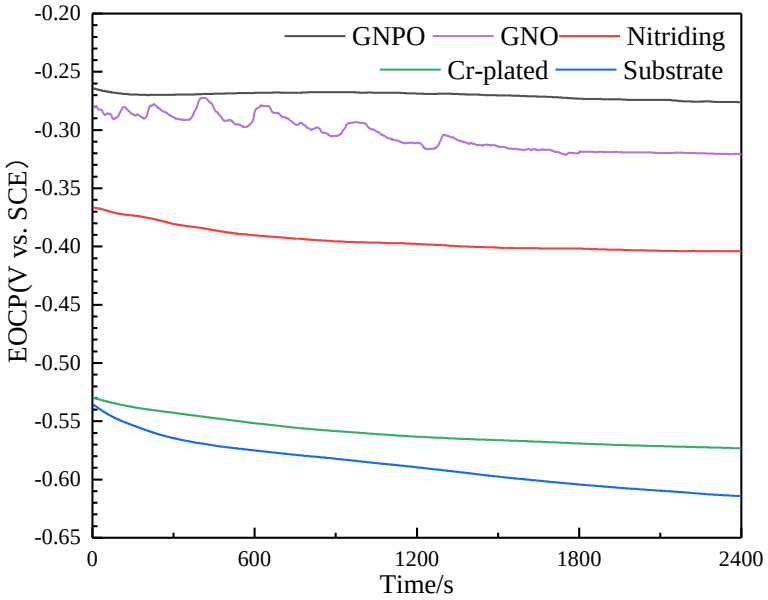

Figure 2. Open circuit potential curves of samples treated with different processes(Effective exposure area: 1 cm^2; Corrosion medium: 3.5%NaCl solution; the potential fluctuation is within 10 mV.)

3.2.2 Potentiodynamic polarization curve

Figure. 3 shows the potentiodynamic polarization curves of samples treated by different processes. Generally, corrosion potential (E_{corr}) and corrosion current density (I_{corr}) are used to characterize the corrosion resistance of the sample surface protection layer. High corrosion potential and low corrosion current density indicate that the layer has good corrosion resistance[11]. As shown in Figure. 3, after gas oxy-nitriding treatment, a significant passivation interval appears in the dynamic polarization anode curve, and in anodic polarization, the current density of chrome-plated and nitriding samples increases more rapidly than that of substrate. The anodic polarization of GNPO sample is faster than that of GNO sample. In the passivation zone, with the increase of potential, the current density of GNPO sample curve decreases more than that of GNO sample curve, indicating that the

oxynitride sample after polishing has better passivation effect and better corrosion resistance of composite permeable layer[12-13]. The potentiodynamic polarization curves are fitted by the Game Echem Analyst software Tafel to obtain the corresponding electrochemical parameters, as can be seen from the table 5, compared to the substrate, the E_{corr} of GNPO sample, GNO sample, nitriding sample and chrome-plated sample were increased by 406 mV, 378 mV, 273 mV and 70 mV, respectively, and the I_{corr} was reduced by approximately 88.6%, 68.7%, 24% and 60.2%, respectively. Samples treated by four different processes have obvious increase, the corrosion resistance of the sample after polishing for oxidation treatment is far better than the other treatment, the corrosion current density and corrosion potential of the unpolished oxynitride sample is slightly lower due to the thicker sparse layer resulting in an uneven thickness of the oxide layer, more porosity and poor densification, this is due to the thick loose lead to uneven thickness of oxide layer, more porosity and density difference, in the corrosion process, Cl^- can reach the compound layer through the pores between the bad oxide layer and produce corrosion effect, and the protection performance is worse than that of the dense oxide layer. Both chrome-plated and nitriding samples show a small area of passivation. Although the corrosion potential of nitriding samples is higher than that of chrome-plated sample, the chrome-plated sample had lower current density and better corrosion resistance. The results of potentiodynamic polarization curve test show that oxidation treatment can greatly improve the corrosion resistance of nitriding sample, and the corrosion resistance of chrome-plated sample is higher than that of nitriding sample but lower than that of oxidation treatment.

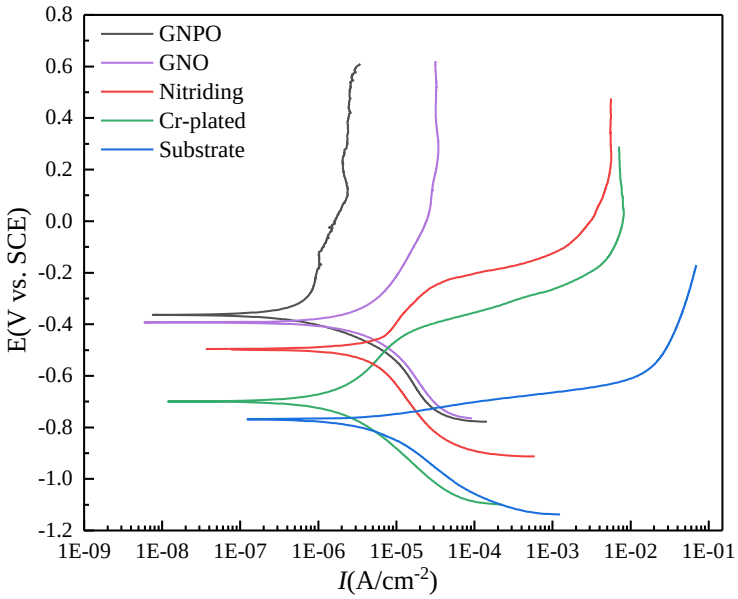

Figure 3. Potentiodynamic polarization curves of samples treated with different processes(The scanning potential is from -400 mV to 800 mV at 10 mV/s scanning rate.)

Table 5. Corrosion potential and corrosion current density polarization parameters of different samples

Sample	E_{corr}（mV）	I_{corr}（μA/cm^2）
GNPO	-363	0.89
GNO	-391	2.45
Nitriding	-496	5.95
Cr-plated	-699	3.12
Substrate	-769	7.83

3.2.3 Electrochemical impedance spectrum

EIS test was performed on samples treated by different processes. After the test, Kramer-Kronig reliability analysis was performed on the data to verify whether the electrode system met the four basic conditions of resistance and absorption [14] : (1) Causality condition: when the electrode system is disturbed by sine wave potential signal, the system responds to the signal. (2) Linear conditions, the amplitude of the disturbance signal of the electrode system is very small, and the response signal approximately conforms to the linear law. (3) Stability condition, when the disturbance signal stops, the electrode system can return to the original state. (4) finiteness, that is, physical quantities that vary with frequency are finite values in all frequency ranges. Table 6 shows the goodness of fit value of K-K relationship curve verification of impedance spectrum. The smaller the value is, the more accurate the measured data results are. The data are verified by Gamry Echem Analyst software. As can be seen from the table, the impedance spectrum measurements of the five samples meet the basic conditions mentioned above, and the goodness of fit value is very small, with the order of magnitude of 10^{-6}.

Table 6. Goodness-of-fit value of impedance spectrum K-K relationship curve verification

Sample	Goodness of Fit(Value)
GNPO	47.09E-6
GNO	88.74E-6
Nitriding	59.42E-6
Cr-plated	45.56E-6
Substrate	12.29E-6

Nyquist curves of 42CrMo steel samples treated by different processes in 3.5% NaCl solution are shown in Figure 4, and Bode diagram is shown in Figure 5. It can be seen from Figure 4 that all Nyquist curves are not perfect arcs, which is closely related to the roughness of the sample surface and the adsorption/decomposition of surface corrosion products. No straight line with slope 1 appears in the low-frequency area of all curves, indicating that Warburg impedance does not appear in the process of corrosion measurement[14]. According to Figure 4, it can be clearly seen that the chrome-plated sample has two capacitance-reactance arcs, while the two capacitance-reactance arcs of the oxygen-nitriding and nitriding samples are not obvious enough, which needs to be analyzed in combination

with the Bode diagram.

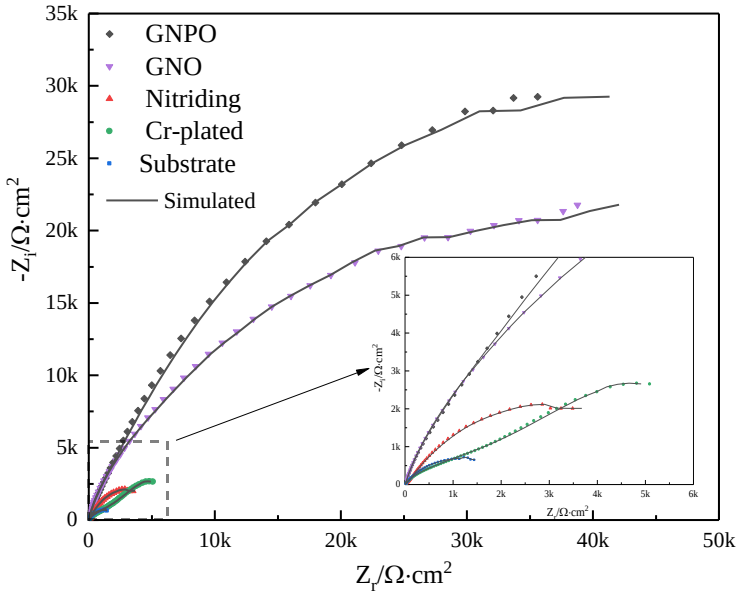

Figure 4. Nyquist curves of samples treated with different processes(Effective exposure area: 1 cm^2; Corrosion medium: 3.5%NaCl solution; The frequency of electrochemical impedance spectrum measurement ranges from 0.01 Hz to 10 KHz)

The Nyquist curve of substrate only has a radius of arc, which indicates that the corrosion is mainly controlled by charge transfer and only has a time constant [15,16]. The radius of arc generally represents the size of charge transfer resistance, so the substrate has the smallest charge transfer resistance and the worst corrosion resistance. The radius of capacitive arc reactance of the two oxygen-nitriding samples near the high frequency region is smaller than that of the chrome-plated samples, and the impedance value is smaller, and the capacitive arc reactance radius of the two oxygen-nitriding samples is much larger than that of the chrome-plated sample in the low frequency region. GNPO sample has the largest capacitive arc radius, indicating that the charge transfer resistance of the sample is the largest. Impedance analysis of experimental results by Nyquist plots alone will produce large errors, so Bode must be taken into account.

Figure. 5 (a) shows the relationship between impedance modulus and frequency, and Figure. 5 (b) shows the relationship between phase Angle and frequency. According to Figure 5 (b), we can see that the phase Angle and frequency diagrams of oxygen-nitriding samples, chrome-plated sample and nitriding samples all have two obvious time constants. In the whole frequency range (0.01Hz-100kHz), the maximum phase Angle amplitude of GNPO samples is close to 75°. The time constant in the high frequency region corresponds to the interface behavior of electrolyte/modified layer, and the time constant in the low frequency region corresponds to the interface behavior of electrolyte/matrix. In figure 5 shows that under the high frequency, the phase Angle is not zero this shows that the working electrode surface defects or vulnerabilities [17]. At low frequencies, the impedance modulus|Z| is in descending order for GNPO, GNO, chrome-plated, nitriding and substrate samples. Combining Figure

4 and Figure 5, the impedance modulus|Z| of GNPO sample is the largest , phase Angle close to 75 °, the low frequency has the biggest platform, the best corrosion resistance, corrosion resistance of chrome-plated sample is better than that of nitriding sample, but inferior to oxygen-nitriding samples, the gas oxygen nitriding process maximizes the corrosion resistance of the substrate.

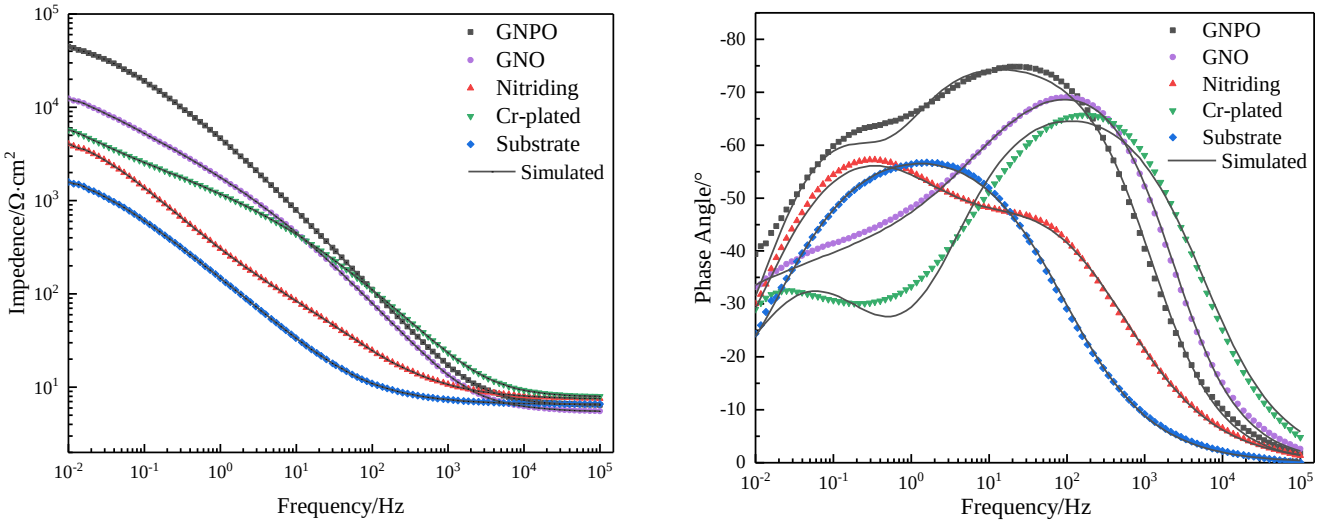

(a) Impedance modulus versus frequency diagram (b) Phase angle versus frequency diagram

Figure 5. Bode diagrams of samples treated with different processes(Effective exposure area: 1 cm^2; Corrosion medium: 3.5%NaCl solution; The frequency of electrochemical impedance spectrum measurement ranges from 0.01 Hz to 10 KHz)

According to the characteristics of electrochemical impedance spectrum, it is fitted with the corresponding electrochemical equivalent circuit. Figure. 6 equivalent circuit model was selected to characterize the electrochemical corrosion system of the sample, in which R_s represents the electrolyte solution resistance, R_{ct} represents the charge transfer resistance, and R_{pl} represents the outer resistance of the modified layer containing defects such as pores and cracks[18]. Considering the deviation from the ideal capacitor, constant phase element (CPE) Q represents the double layer capacitance. Qpl and Qdl respectively represent the capacitance of the outer layer of the modified layer and the capacitance of the double electric layer of the dense layer and electrolyte, and their impedance Z_Q expression[13] is ：

$$Z_Q = \frac{1}{Y_0} \cdot (j\omega)^{-n} \quad (1\text{-}1)$$

Y_0—basic admittance of double layer capacitance ($S \cdot S^n \cdot cm^{-2}$);

n — Constant related to the surface of the double electric layer (n=0, representing pure resistance; n =1, representing ideal capacitance);

ω — Angular frequency (Hz).

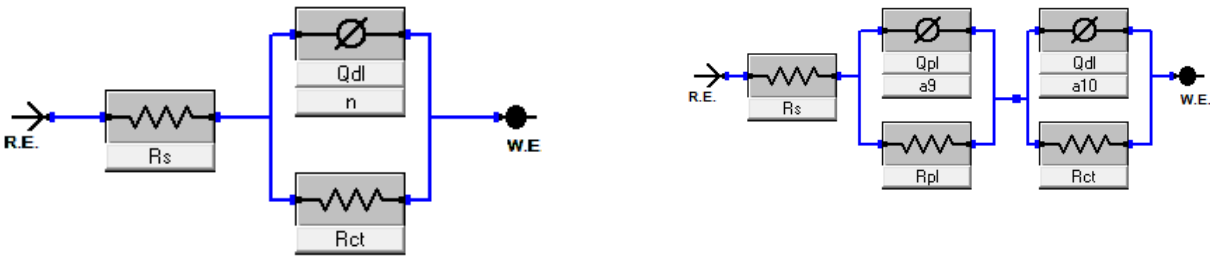

(a) Equivalent circuit model of substrate (b) Equivalent circuit model of modified layer

Figure 6. Equivalent circuit model fitted to EIS data

The EIS of the substrate was fitted according to the equivalent circuit in Figure 6 (a), and the EIS of the sample after modification was fitted by the equivalent circuit in Figure 6 (b). The fitting results of equivalent circuits corresponding to different samples in NaCl solution are listed in Table 5, and the errors of all components are less than 10%. The value of electrolyte resistance R_s is very small and plays a negligible role in the corrosion reaction process. As can be seen from Table 7, the corrosion resistance of the substrate is the worst, followed by the nitriding layer. The corrosion resistance of the chromium plated coating is between the nitriding sample and the oxygen-nitriding sample, which is consistent with the experimental results of the dynamic polarization curve. The charge transfer resistance of the GNPO sample is 50550 $\omega \cdot cm^2$, and the resistance of the modified layer is 6742 $\omega \cdot cm^2$. Higher than chrome-plated 8444 $\omega \cdot cm^2$ and 931.8 $\omega \cdot cm^2$. Due to the loose layer of compound outer layer, the anions in solution can pass through these defects and reach the dense compound layer, which is also the main anticorrosive permeable layer. The R_{pl} of the chrome-plated sample is larger than that of the nitriding sample due to the existence of a thin passivation film on the surface of the chrome-plated sample. After the passivation film fails, the anions in the solution contact with the substrate surface through cracks on the surface of the chrome-plated sample. 42CrMo steel surface oxidation reaction, the dissolution of iron constantly produces Fe^{2+} and OH^- in solution to form Fe $(OH)_2$ corrosion products film. These corrosion products will temporarily block the cracks and delay the corrosion rate, so that the R_{ct} is slightly higher than the nitriding sample, and the corrosion resistance is better than the nitride process. The R_{pl} and R_{ct} of GNPO samples are both at maximum values. Due to polishing, on the one hand, the thickness of the loose layer in the outer layer of the compound layer is reduced, and on the other hand, the post-oxidation oxidation is conducive to filling these loose Spaces, and the surface oxidation layer is denser and smoother. The corrosion of the oxygen-nitriding samples occur first on the outermost oxide layer. When the oxide layer is corroded, the compound layer will continue to protect the substrate, which will greatly slow down the corrosion rate and significantly improve the corrosion resistance of the specimen. The GNPO sample has better corrosion resistance due to the superiority of the compound modified layer on the surface than the GNO sample.

Table 7. EIS equivalent circuit fitting results

Sample	R_s	Qdl	n	R_{pl}	Qpl	n1	R_{ct}
	$\Omega \cdot cm^2$	$S \cdot sn \cdot cm^{-2}$		$\Omega \cdot cm^2$	$S \cdot sn \cdot cm^{-2}$		$\Omega \cdot cm^2$
GNPO	7.7	1.01E-4	0.68	6742	0.61E-4	0.79	50550
GNO	5.35	3.22E-4	0.75	1511	0.98E-4	0.83	17200
Nitriding	7.45	1.53E-4	0.87	631.4	8E-4	0.64	7272
Cr-plated	7.23	6.65E-4	0.65	931.8	1.06E-4	0.74	8444
Substrate	6.6	1.93E-3	0.69		—		2282

3.2.4 Corrosion morphology

The surface corrosion morphology of samples after polarization reaction treated by different processes are shown in Figure 7. It can be seen from Figure. 7 (a) that the 42CrMo steel substrate has uneven surface after corrosion, and circular holes with multi-point corrosion appear. Local pitting corrosion occurs on the matrix surface continuously induced and promoted by Cl^-. With the increase of H^+ in the etching hole [19-21], PH decreases and the acidification of the solution in the hole keeps the metal in the hole in active dissolution state, further corrosion in the hole, thus forming pitting corrosion. Figure 7(b) shows the surface morphology of the nitriding sample after corrosion. There are still many shallow pits and a few holes on the surface. Some large pores in the loose layer will cause local pitting in this area. Figure 7(c) shows the corroded surface of the chrome-plated sample. Many spot-like corrosion spots and strip-like patterns appear on the surface of the chromium coating, which is due to the existence of micro-cracks on the surface of the chromium coating[22-24], the substrate is corroded by the solution at the cracks, forming strip-like patterns on the surface, and large corrosion spots appear locally. Figure 7(d) and 7(f) show the corrosion surface morphology of GNO and GNPO samples, respectively. In Figure 7(d) it is clear that there are more pitting corrosion pits on the oxide surface, in Figure 7(f) there are no obvious pitting corrosion pits, only a few corrosion marks in the surface recesses or scratches.

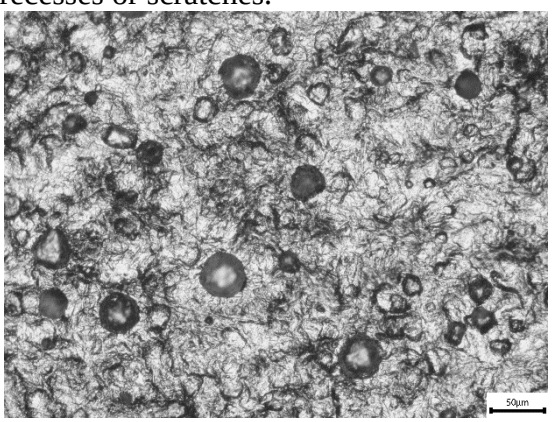

（a）Substrate

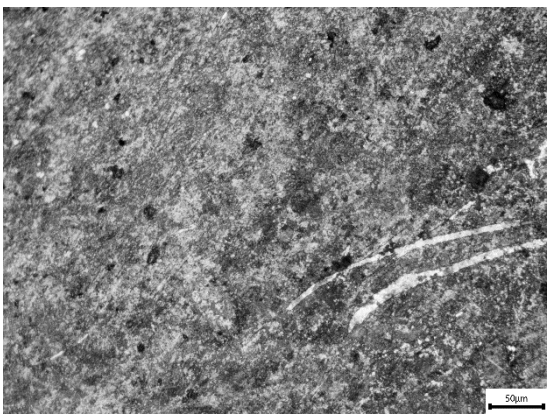

（b）Nitriding sample

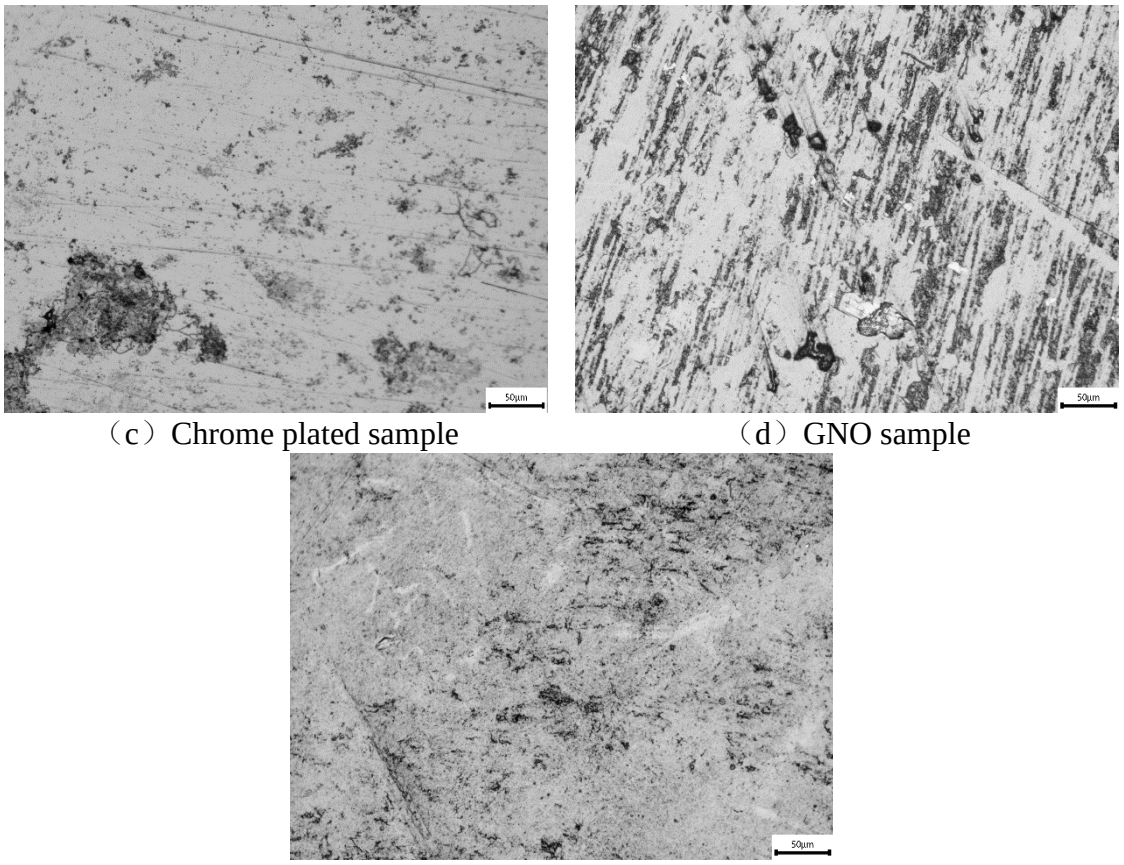

（c）Chrome plated sample （d）GNO sample

（e）GNPO sample

Figure 7. Surface corrosion morphology of samples treated by different technologies(Magnification: 200x)

4.CONCLUSIONS

The surface of the chrome-plated sample forms a bright white chromium coating of about 22 μm, and the boundary between the trivalent chromium electroplating sample and the substrate is clear and there are obvious gaps. The total thickness of oxide layer and compound layer of GNO sample is 20.89 μm, and that of GNPO sample is 18.56 μm. The compound layer has the effect of improving wear resistance and anticorrosion. The corrosion resistance of the samples after the different processes in order of strength to weakness are GNPO sample, GNO sample, chrome-plated sample, nitrided sample and substrate.The E_{corr} of corrosion potential and I_{corr} of corrosion current density of GNPO sample are -363 mV and 0.89 μA/cm^2 respectively, showing the best corrosion resistance.

ACKNOWLEDGEMENTS
This research was financially supported by the Municipal University Cooperation Fund Project of Yangzhou (No. YZ2021151 and No. YZ2021155).

References

1. W.S. Singh, N. Srilatha, *Mater. Today*., 5(2)(2018)4832-4837.
2. C.C. Alvarez, M.G. Bravo,A.Z. Hernández, *J Trace Elem Med Biol*., 65(2021)126729.
3. C.A. Huang, Y.W. Liu, C.H. Chuang, *Thin Solid Films*., 517.17(2009)4902-4904.
4. C.W. Liao, H.B. Lee, K.H. Hou, S.Y. Jian, C.E. Lu, M.D. Ger, *Electrochim. Acta*., 209(2016)244-253.
5. H.R. Abedi, M. Salehi, M. Yazdkhasti, *Electron. Mater. Lett*., 64.6(2010)698-701.
6. D.L. Snyder, *Trans. Inst. Met. Finish*., 110.2(2012)14-21.
7. S. Mahdavi, S.R. Allahkaram, *J.Alloys.Compd*., 635(2015)150-157.
8. M.S. Doolabi, S.K. Sadrnezhaad, D.S. Doolabi, *Anti-Corros Method M*., 61.4(2014) 205-214.
9. B.S. Li, A. Lin, F.X. Gan, *Surf. Coat. Technol*., 201.6(2006)2578-2586.
10. D.S. Li, K. Chen, X.Q. Fu, M. Kang, Z.X. Hua,X.F. Wang, *Int. J. Electrochem. Sci*., 16 (2021) 210233
11. H. Wang, J. Liu, D.W. Gu, D. Zhu, *Int. J. Electrochem. Sci*., 15 (2020) 9313.
12. S. Wang, Y. Wang, Y. C. Zou, Y. F. Wu, G. L. Chen, J. Hu , O. Yang, *Chem. Eng. J*., 402 (2020) 126116.
13. Y. Wan, Y. Yu, L. Cao, M. Zhang, J. Gao , C. Qi, *Surf. Coat. Technol*., 307 (2016) 316.
14. E.E.D. Obaldia, S. Herrera, L.K. Grunenfelder, D.Kisailus, P.Zavattieri, *J Mech Phys Solids*., 96(2016)511-534.
15. Y.W. Cao, C.S. Guo, D.T. Wu, Y. Zou, *J. Alloy. Compd*., 867 (2021) 159126.
16. J.S. Chen, C. Yu, H. Lu, *J. Alloy. Compd*., 625(2015)224-230.
17. E. Boztepe, A.C. Alves, E. Ariza, L.A. Rocha, N. Cansever, F. Toptan, *Surf. Coat. Technol*., 334 (2018) 116-123.
18. Z.Y. Gong, R.F. Chen, J. Li, P. Cao, H.R. Geng, *Int. J. Electrochem. Sci*., 15 (2020) 1117-1127.
19. T. Yamashita, P. Hayes, *Appl. Surf. Sci*., 254.8(2008) 2441-2449.
20. S.M.R. Niya, M. Hoorfar, *J. Power Sources*., 240(2013) 281-293.
21. R.D. Evans, C.H.H .Jr, Y.S. Kang, G.L.Doll, *Tribol. Trans*., 58.3(2015)444-453.
22. L. Zhang, C. Ren, Q. Yu, J.Zhang, S.Q. Sun, Q.S. Ren, Y. Lian, X.L. Chen, W. Gao, *Surf. Coat. Technol*., 315(2017)95-104.
23. N. Vidakis, A. Antoniadis, N. Bilalis, *J Mater Process Technol*., 143-144.1(2003)481-485.
24. M. Sadeghi-dehsahraee, P. Najafisayar, *J. Mater. Eng. Perform*., 28(9)(2019)5674-90.